Cellular and Molecular Life Sciences (2018) 75:4403–4416
https://doi.org/10.1007/s00018-018-2885-x

ORIGINAL ARTICLE

Crosstalk between FGF23- and angiotensin II-mediated Ca^{2+} signaling in pathological cardiac hypertrophy

Ketaki N. Mhatre[1,2] · Paulina Wakula[1] · Oliver Klein[1] · Egbert Bisping[2] · Jakob Völkl[1] · Burkert Pieske[1,3,4] · Frank R. Heinzel[1,3]

Received: 3 January 2018 / Revised: 16 July 2018 / Accepted: 19 July 2018 / Published online: 30 July 2018

Abstract

Heart failure (HF) manifestation and progression are driven by systemic activation of neuroendocrine signaling cascades, such as the renin–angiotensin aldosterone system (RAAS). Fibroblast growth factor 23 (FGF23), an endocrine hormone, is linked to HF and cardiovascular mortality. It is also a mediator of left-ventricular hypertrophy (LVH). In vivo, high circulating levels of FGF23 are associated with an altered systemic RAAS response. FGF23 is proposed to trigger pathological signaling mediated by Ca^{2+}-regulated transcriptional pathways. In the present study, we investigated Ca^{2+}-dependent signaling of FGF23 in ventricular cardiomyocytes and its association with angiotensin II (ATII). In neonatal rat ventricular myocytes (NRVMs), both ATII and FGF23 induced hypertrophy as observed by an increase in cell area and hypertrophic gene expression. Furthermore, FGF23 activates nuclear Ca^{2+}-regulated CaMKII–HDAC4 pathway, similar to ATII. In addition to a global increase in cytoplasmic Ca^{2+}, FGF23, like ATII, induced inositol 1, 4, 5-triphosphate (IP3)-induced Ca^{2+} release from the nucleoplasmic Ca^{2+} store, associated with cellular hypertrophy. Interestingly, ATII receptor antagonist, losartan, significantly attenuated FGF23-induced changes in Ca^{2+} homeostasis and cellular hypertrophy suggesting an involvement of ATII receptor-mediated signaling. In addition, application of FGF23 increased intracellular expression of ATII peptide and its secretion in NRVMs, confirming the participation of ATII. In conclusion, FGF23 and ATII share a common mechanism of IP3-nuclear Ca^{2+}-dependent cardiomyocyte hypertrophy. FGF23-mediated cellular hypertrophy is associated with increased production and secretion of ATII by cardiomyocytes. These findings indicate a pathophysiological role of the cellular angiotensin system in FGF23-induced hypertrophy in ventricular cardiomyocytes.

Keywords Cardio-renal axis · Ventricle cardiomyocytes · Local renin-angiotensin system · Autocrine · Nuclear Ca^{2+} signaling

Introduction

Left-ventricular hypertrophy (LVH) is a common myocardial structural anomaly associated with heart failure (HF). Cardiac hypertrophy is commonly accompanied by complex changes that include an increase in cardiomyocyte size, re-expression of fetal cardiac genes, and dysregulation of cardiomyocyte Ca^{2+} homeostasis [1]. LVH serves as a diagnostic and prognostic marker of cardiac remodeling as seen in HF. Chronic kidney disease (CKD) is a highly prevalent co-morbidity in HF and serves as a trigger for LVH. Kidney dysfunction mediates the development of HF through activation of systemic RAAS with an increase in angiotensin II (ATII) levels [2]. ATII is a well established, and a strong trigger of cardiac hypertrophy and remodeling acting via inositol trisphosphate (IP3)-mediated Ca^{2+}-dependent

Electronic supplementary material The online version of this article (https://doi.org/10.1007/s00018-018-2885-x) contains supplementary material, which is available to authorized users.

✉ Frank R. Heinzel
frank.heinzel@charite.de

[1] Department of Internal Medicine and Cardiology, Charité University Medicine, Campus Virchow-Klinikum, 13353 Berlin, Germany

[2] Department of Cardiology, Medical University Graz, Auenbruggerplatz 15, 8036 Graz, Austria

[3] German Center for Cardiovascular Research (DZHK), Berlin, Germany

[4] Department of Internal Medicine and Cardiology, German Heart Center, 13353 Berlin, Germany

signaling pathways. In our earlier work, we have shown that the nuclear envelope (NE) acts as a functional Ca^{2+} store and that altered nuclear Ca^{2+} signaling occurs early in cardiac hypertrophy [3]. IP3-induced Ca^{2+} release (IICR) by stimulation of IP3R expressed on the NE is important for nuclear Ca^{2+}-mediated CaMKII-dependent HDAC4 phosphorylation and induction of hypertrophy-related fetal gene program [4–6].

During CKD, an increase in the circulating levels of fibroblast growth factor 23 (FGF23) occurs. FGF23 is a hormone secreted by osteocytes, and a central endocrine regulator of circulating phosphate and Ca^{2+} homeostasis [7]. Several large epidemiological studies have demonstrated that elevated serum levels of FGF23 independently correlate with increased incidence and prevalence of LVH [8].

Application of FGF23, in vitro on primary cultures of ventricular cardiomyocytes, alters Ca^{2+} homeostasis by increasing Ca^{2+} influx via L-type Ca^{2+} channels and modulates sarcoplasmic reticulum (SR) Ca^{2+} pump (SERCA) activity [9, 10]. The effects of FGF23 on IP3-dependent nuclear Ca^{2+} release related to hypertrophic gene regulation, however, have not yet been studied.

In our present study, we provide novel evidence for a crosstalk between FGF23 and ATII-triggered nuclear Ca^{2+}-mediated signaling in cardiac hypertrophy.

Methods

Isolation and culture of neonatal rat ventricular cardiomyocytes

Neonatal rat ventricular cardiomyocytes (NRVMs) were isolated from 1–3 day old rat pups and cultured for a period of 5 days as previously described [11]. In brief, neonatal rat hearts were excised and placed in ice-cold PBS. Blood and connective tissues were removed and ventricles minced. Cells were dissociated by five rounds of digestion at 37 °C for 10–12 min in digestion buffer containing Liberase™ (80 µg/ml), Trypsin (0.1%; Life Technologies, Carlsbad, CA, USA), and DNase I (20 µg/ml) in 10-µM Ca^{2+}–1× HBSS-buffered solution. The dissociated cells of each round of digestion were treated with 10% horse serum (Life Technologies, Carlsbad, CA, USA) and centrifuged. The cell pellets were re-suspended in culture medium-containing DMEM-F12 medium (Thermo Scientific, Rockford, IL, USA) with 10% fetal bovine serum (VWR International, PA, USA) and 1% penicillin/streptomycin (100 units/ml) and kept on ice. Pooled cells were passed through a cell strainer (100 µm) and further pre-plated for 1 h for cardiomyocyte enrichment to remove contaminating fibroblasts. Cardiomyocytes were seeded at a density of $0.5–1 \times 10^6$ cells/ml on 1% gelatinized cell culture and imaging dishes. Cells were cultured in culture medium at 37 °C in a humidified atmosphere containing 5% CO_2. Culture medium was changed to serum-free medium-containing 80% DMEM-F12 and 20% M199 GlutaMAX Supplement (Thermo Scientific, Rockford, IL, USA) with 1% penicillin/streptomycin (100 units/ml) after 24 h. Myocytes were cultured under serum-free conditions for 48 h before experiments. Agonist stimulation was done on day 4 post-isolation, with either ATII (1 µM) or FGF23 (25 ng/ml; R&D Systems). Protease Inhibitor Cocktail (1:400) was used in our cell culture to prevent proteolytic degradation of peptides (e.g., ATII). In some experiments, myocytes were treated with Losartan (1 µM), 2-aminoethoxydiphenyl borate (2-APB, 5–10 µM), Xestospongin.C. (Xest.C., 10 µM), or vehicle (DMSO) 30 min (control) before and during agonist stimulation.

Real-time quantitative RT-PCR

To investigate upstream hypertrophic signaling pathways, we quantified classical marker gene for cardiac hypertrophy and fibrosis, ACTA-1, at an early time-point following the hypertrophic triggers. We also measured the calcineurin reporter gene, RCAN-1, which is involved in Ca^{2+}-dependent cardiac hypertrophic signaling [12]. After the stimulus, total RNA was isolated from the single wells of the 6-well plates at suitable time-point using the RNeasy Mini Kit (Qiagen, Hilden, Germany), including DNase treatment. Quality and quantity of RNA were assessed with a Nanodrop 1000 spectrophotometer (Thermo Fischer Scientific, Wilmington, DE, USA) and reverse transcription was performed with QuantiTect ReverseTranscription Kit (Qiagen, Hilden, Germany). qPCR was carried out using SYBR Green Mastermix (Bio-Rad, Hercules, CA, United States) in 10-µl total reaction volumes on a LightCycler® 480 Instrument II at optimized thermocycling settings. Relative gene expression was calculated using the ddC_t method, with expression normalized to GAPDH (RPL-4) as a reference gene. Each sample was run in triplicates and fold changes were calculated in comparison with the corresponding control (vehicle-treated NRVMs). Sequences of used primer oligonucleotides are provided in Supplementary Table S1.

Western blot (WB)

Neonatal rat ventricular myocytes were homogenized at 4 °C in cell lysis buffer with freshly added protease inhibitors (PMSF, leupeptin, aprotinin, pepstatin A). Lysates were run on 4–12% Bis–Tris polyacrylamide gels and transferred to nitrocellulose membranes for 2 h. Proteins on the membrane were stained with Ponceau S. Non-specific binding was blocked with 3% Bovine serum albumin in Tris-buffered saline (pH 7.4) containing 0.1% Tween-20. Membranes were probed with anti-HDAC4 phosphoS632 and anti-HDAC4

(Abcam, Cambridge, USA) sequentially, overnight at 4 °C. Anti-rabbit IgG linked with IRDye 800CW (pHDACS632) and anti-rabbit linked with 680RD (HDAC-4) (LI-COR, Nebraska, USA) were used as a secondary antibody. The signal was detected with Odyssey CLx System. The band intensities were determined by Image Studio software (LI-COR).

Ca^{2+} measurements

Cultured NRVMs were washed with Normal Tyrode Solution (NT) (1.8-mM $CaCl_2$). Cells were loaded with the 20-µM Fluo 4AM (Molecular Probes, Eugene, OR, USA), the Ca^{2+}-sensitive fluorescent dye, in NT together with 20% (w/v) Pluronic-127/dimethyl sulfoxide (DMSO) (Life Technologies, Carlsbad, CA, USA). To ensure similar loading of the cardiomyocytes, we incubated the cells for exactly 30 min in dark at room temperature [13]. Cells were then washed twice with NT for 15 min for de-esterification and used for Ca^{2+} imaging.

Intracellular Ca^{2+} recordings in cytosol and nucleus were performed using a confocal laser-scanning microscope (ZEISS LSM 800) that consisted of an inverted microscope equipped with a 40× oil-immersion objective lens. Fluo-4 was excited by the 488-nm light from an argon-ion laser and fluorescence was collected at wavelengths > 515 nm [13]. The temporal resolution of the scanning was 0.58–0.8 ms per line. The confocal line was set in parallel to the long axis of the cardiomyocyte crossing the middle of the nuclei for the recording of the $[Ca^{2+}]$ in the cytoplasm as well as nucleus. Cells were field-stimulated via two platinum electrodes at 1 Hz. Steady-state CaTs were recorded at room temperature. For analysis, 4–5 consecutive transients were averaged using custom-made algorithms coded in IDL (IDL 7.0, ITT Visual Information Solutions, Paris, France) as previously described [13, 14]. $[Ca^{2+}]$-dependent fluorescence (F) was normalized to F averaged during 30 ms before the onset of Ca^{2+} transient ($F0$). Total cytosolic or nuclear Ca^{2+} load during a paced beat was calculated as the area under the curve (AUC) of the normalized Ca^{2+} transient (CaT). Ca^{2+} sparks were analyzed using SparkMaster [15]. NRVMs were treated with ATII (1 µM) or FGF23 (25 ng/ml) in NT solution or (vehicle added) NT solution for the duration of 15–90 min. A subset of NRVMs was treated with Losartan (1 µM), 2-APB (5–10 µM), Xest.C. (10 µM), or vehicle (DMSO) 30 min before agonist stimulation.

Immunocytochemistry (ICC) analysis

Cardiomyocyte size measurements

NRVMs were fixed with methanol/acetone (ratio 1:1, at − 20 °C), permeabilized for 5 min with phosphate-buffered saline (PBS) containing 0.1% Triton X-100 and 0.1% Na-citrate, and blocked with 5% bovine serum albumin in PBS for 1 h. Cells were incubated with primary antibody for cardiomyocyte-specific sarcomeric desmin (mouse monoclonal antibody, 1:50, Dako Cytomation, Denmark) overnight at 4 °C in the same solution as blocking solution. Cells were incubated with the secondary AlexaFluor® 488-conjugated antibody (rabbit anti-mouse IgG, 1:1000, Invitrogen, CA, USA) for 45 min in dark at RT. Nuclei were stained with DAPI. NRVMs were visualized with an inverted fluorescence phase-contrast microscope (BZ-9000E, All-in-One fluorescence microscope, Keyence, Osaka, Japan), and images were captured using a digital camera CFI60 (Nikon, Tokyo, Japan). The cell surface area of desmin-positive cardiomyocytes were analyzed from at least 20 fields randomly chosen in each imaging dish (ImageJ, NIH, USA).

Intracellular angiotensin expression

Methanol/acetone fixed NRVMs were co-stained with the anti-desmin antibody (1:50, Dako Cytomation, Denmark) and anti-angiotensin II/angiotensinogen antibody (1:50, angiotensin (N-10), Santa Cruz Biotechnology, CA, USA) as specified in protocol above. Along with FGF23 (25 ng/ml) treatment, we used high glucose (25 mM) treatment as a positive control for induction of ATII expression in cardiomyocytes [16]. All other conditions (negative control, vehicle-treated control, and FGF23) were in 10 mM glucose medium. Intracellular ATII expression in NRVMs was visualized using confocal laser-scanning microscope (ZEISS LSM 800, Carl Zeiss, Oberkochen, Germany) with a 40× oil-immersion objective lens. A field of vision with 2–3 NRVMs was chosen. Using confocal microscopy, a z-stack of five adjacent layers was recorded enclosing the equatorial plane. z-stacks were recorded with a voxel size of 0.078 µm in xy and 1.0 µm in z-axis. The equatorial plane of each of the scanned cardiomyocyte for every condition with identical settings for excitation and detection was analyzed. Images were converted to binary by thresholding with a signal threshold defined as mean + 3 standard deviations of the intracellular intensity in negative controls (without primary antibody). Expression was quantified as the fraction of signal-positive voxels and was given as a percentage of the sampled cell volume.

Mass spectrometry

The supernatants were dried in a speedvac (Eppendorf, Hamburg, Germany) and re-suspended in 1 ml 0.1% trifluoroacetic acid. 100 µl sample solution was desalted and peptides concentrated using ZipTip (C18) according to the standard manufacturer protocol (Merck Millipore, Billerica, MA, USA). The resulting peptide mixtures were then spotted on one 384-anchor-containing MALDI AnchorChip targets

(Bruker Daltonic, Bremen, Germany) and mixed with a 1 µl matrix solution and analyzed. MALDI-IMS data acquisition was performed in positive-ion reflector mode on an Autoflex III MALDI-TOF/TOF using flexControl 3.0 software (Bruker Daltonic). Measurement settings were as follows: detection range of *m*/*z* 800–3000, 200 laser shots per spot, and the sampling rate of 2.0 GS/s.

Solutions and chemicals

All chemicals were obtained from Sigma-Aldrich (St. Louis, MO, USA) unless noted otherwise. Cell lysis buffer contained (in mM): 20 Tris pH 7.5, 150 NaCl, 1 Na_2EDTA pH 8, 1 EGTA pH 7, 1% Triton, 2.5 $Na_4P_2O_7$, 1 Na_3VO_4, and 1 β-glycerophosphate. Normal Tyrode solution (NT) contained (in mM): 130 NaCl, 4 KCl, 1.8 $CaCl_2$, 1 $MgCl_2$, 10 D-glucose, and 10 HEPES; pH 7.4 with NaOH. Matrix solution contained: 1 ml 7 g/l a-cyano-4-hydroxycinnamic acid (Bruker Daltonic) in 50% acetonitrile (Fluka, St. Louis, USA) and 1% trifluoroacetic acid (spectroscopy purity, Merck, Darmstadt, Germany).

Statistical analysis

Primary cell culture experiments were conducted on 3–5 independent cell culture isolates obtained on different days with technical replicates. The appropriate statistical analysis was performed using paired or unpaired *t* test or Mann–Whitney *U* test (for two groups), and ANOVA or Kruskal–Wallis followed by Bonferroni or Dunn's test for multiple comparisons (for three or more groups). Chi-square test was used to compare nuclear spark incidence between the treatment groups. Statistical tests were performed using SPSS (IBM SPSS Statistics for Windows, Version 23.0. Armonk, NY, USA: IBM Corp, USA). Results are reported as a mean ± standard error of the mean (SEM) or standard deviation (SD), and a P value < 0.05 was considered significant. N is the number of independent isolation, and n is the number of individual cells analyzed.

Results

FGF23 induces cellular hypertrophy and activates hypertrophy-related genes in neonatal rat ventricular cardiomyocytes

We compared the response of isolated neonatal rat ventricular cardiomyocytes (NRVMs) to treatment with FGF23 or ATII for 48 h with vehicle-treated control NRVMs (Fig. 1). An increase in cell surface area in response to ATII (46.8 ± 2.6%; $P < 0.01$) and FGF23 (37.4 ± 2.5%; $P < 0.01$) treatment was observed as compared to control cells from five independent isolations with > 1000 cells analyzed per

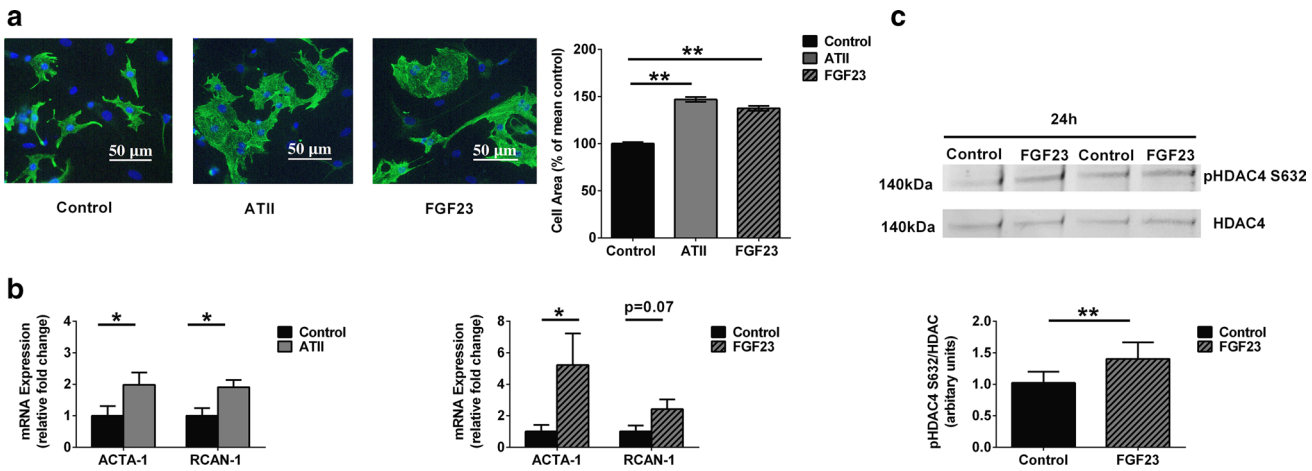

Fig. 1 Hypertrophic response to ATII and FGF23 treatments. **a** Representative images of isolated NRVMs after 48-h treatment ATII and FGF23, as revealed by immunocytochemical analysis using antibodies to cardiomyocyte-specific Desmin (green) and DAPI (blue) used to identify nuclei (scale bar: 50 µm). The bar graphs shows relative percentage change in cell area which was analyzed compared with that of vehicle-treated control cells (black) for 48 h of treatment of NRVMs with ATII (grey) and FGF23 (pattern) (mean ± SEM; $N = 5$ independent isolations; $n > 1000$ cells per group; $^{**}P < 0.01$, compared with control cells; Kruskal–Wallis followed by Dunn's test). **b** Compared to control cells (black), expression of genes ACTA-1 and RCAN-1 at 1 h of ATII treatment (left) (grey). Compared to control cells (black), expression of genes ACTA-1 and RCAN-1 at 6 h of FGF23 treatment (right) (pattern) (mean ± SEM; $N = 5$ independent isolations quantified by RT-PCR normalized to GAPDH gene expression; $^{*}P < 0.05$, compared with corresponding control; unpaired *t* test or Mann–Whitney *U* test). **c** Degree of phosphorylation of HDAC4 at Serine 632 site was examined by immunoblot (above) in NRVMs treated with FGF23 vs. control at 24 h time-point. The bar graph (below) is from $N = 6$ independent isolations (mean ± SEM; $^{**}P < 0.01$, compared with vehicle-treated control cells; paired *t* test)

conditions (Fig. 1a). Expression of pro-hypertrophic genes, ACTA-1 and RCAN-1, were compared for both ATII and FGF23 treatment with control cells using GAPDH as a housekeeping gene. GAPDH normalized to RPL-4 showed stable expression in all our treatment groups (Fig. S1). Following application of ATII, the hypertrophy-marker genes ACTA-1 and RCAN-1 were elevated after 1 h of treatment (Fig. 1b). FGF23 application resulted in an increase in ACTA-1 at 6 h of stimulation (Fig. 1b).

Next, we investigated the phosphorylation state at site Serine 632(S632) of HDAC4, which is known to be activated by ATII [17]. In cardiomyocytes, upon stimulation by a hypertrophic trigger like ATII, nuclear Ca^{2+}-CaMKII has been shown to tightly regulate epigenetic processes controlled by class II histone deacetylases (e.g., HDAC4) leading to transcriptional activation of gene programs that drive pathological remodeling [4]. Using immunoblotting, we observed a significant increase of 1.4 ± 0.1 fold in S632 phosphorylation of HDAC4 (140 kDa) in FGF23-treated cells for 24 h as compared to that of vehicle-treated control cells from six independent NRVM isolations (Fig. 1c).

These results confirm that both ATII and FGF23 act as a hypertrophic trigger in our cardiomyocyte culture. Based on the data from the previous studies and observations made in the present study, it could be possible that both, FGF23 and ATII, share similar Ca^{2+}-mediated hypertrophic signaling pathways.

ATII and FGF23 acutely increase cytoplasmic as well as nuclear Ca^{2+}

To examine the effects of FGF23 on cytosolic and nuclear Ca^{2+} compared to ATII, we investigated Ca^{2+} signals in cytoplasm and nucleus of NRVMs electrically stimulated at 1 Hz as exemplified in Fig. 2a. Following an acute treatment (15–90 min), the cytosolic CaT amplitude increased by 2.0 ± 0.6-fold with FGF23 ($P < 0.01$) and tended to increase by 1.7 ± 0.3-fold with ATII ($P = 0.05$). Interestingly, FGF23 significantly increased the nuclear CaT amplitude, again with a similar trend with ATII (Fig. 2b).

The area under the curve (AUC) of the CaT is a function of the total intracellular Ca^{2+} exposure during one Ca^{2+} cycle, and depends not only on the CaT amplitude but also on the Ca^{2+} release and decay kinetics. A substantial increase in AUC was elicited by FGF23 and ATII in both cytosol and nucleus (Fig. 2c). Cytoplasmic CaT AUC increased by 2.9 ± 0.3-fold ($P < 0.01$) with FGF23 and 2.4 ± 0.4-fold ($P < 0.01$) with ATII treatment. Moreover, nuclear CaT AUC increased by 4.3 ± 0.5-fold ($P < 0.01$) with FGF23 and 3.8 ± 0.5-fold ($P < 0.01$) with ATII treatment (Fig. 2c). Thus, both hormones enhanced cytoplasmic as well as nuclear Ca^{2+} exposure.

In addition, we also tested spontaneous spark activity in both the compartment for all the treatment groups. Significantly, more cells in FGF23 and ATII treatment groups exhibited nuclear sparks as compared to control cells (Fig. S2a, b). Ca^{2+} spark frequency was significantly increased in the nucleus of FGF23-treated cells vs. that of control cells but not in the cytoplasm (Fig. S2c). Thus, these results suggest an increase in specifically nuclear Ca^{2+}-release events with ATII or FGF23 treatment of NRVMs.

Role of IP3 in FGF23-induced changes in nuclear Ca^{2+} signal

The nuclear Ca^{2+} transient in ventricular cardiomyocytes is constituted of two components, passive cytoplasmic Ca^{2+} diffusion through nuclear pore complexes and active IP3-induced nuclear Ca^{2+} release (IICR) [18]. To detect a selective effect of stimuli on nuclear Ca^{2+} release independent of cytoplasmic Ca^{2+} diffusion, we normalized the nuclear CaT parameters to corresponding cytoplasmic CaT [19]. The ratio of nuclear-to-cytosolic CaT amplitudes was unchanged with both the treatments (Fig. S3b). However, the ratio of nuclear CaT AUC-to-cytosolic CaT AUC revealed an increase in local nuclear Ca^{2+} release for both FGF23 and ATII (Fig. 3b).

Next, membrane permeable blockers of IP3 receptor, 2-APB (5–10 μM), and Xest.C.(10 μM), were used to investigate the role of IP3 in this augmented nuclear Ca^{2+} release due to ATII or FGF23 treatment. At this concentration, 2-APB did not have any effect on cytosolic CaT amplitude (Fig. S3a), thus making its proposed interference with sarcoplasmic reticulum Ca^{2+} pump not relevant in this study [20]. 2-APB reduced the augmented Ca^{2+} release into the nucleus induced by FGF23 (Fig. 3a, b). However, pretreatment Xest.C. offsets both, FGF23- induced increase in cytoplasmic as well as nuclear Ca^{2+} release with respect to CaT amplitude and CaT AUC (Fig. S4).

Overall, these results suggest that, irrespective of cytosolic Ca^{2+} changes, FGF23-triggered enhancement of nuclear Ca^{2+} signaling is mediated by IICR (Fig. 3b).

Role of ATII/AT1R in FGF23-mediated hypertrophy

As illustrated earlier, FGF23 had similar effects as ATII on NRVMs with respect to cellular hypertrophy and Ca^{2+} homeostasis changes. This raises the intriguing possibility of involvement of ATII signaling in FGF23-induced hypertrophy. To investigate whether there is an overlap between FGF23 and ATII/AT1R signaling, we used losartan, an AT1R antagonist.

Losartan (1 μM) attenuated the FGF23-mediated increase in CaT amplitude as well as the total Ca^{2+} (CaT AUC) released into the cytosol and nucleus (Fig. 4a, b),

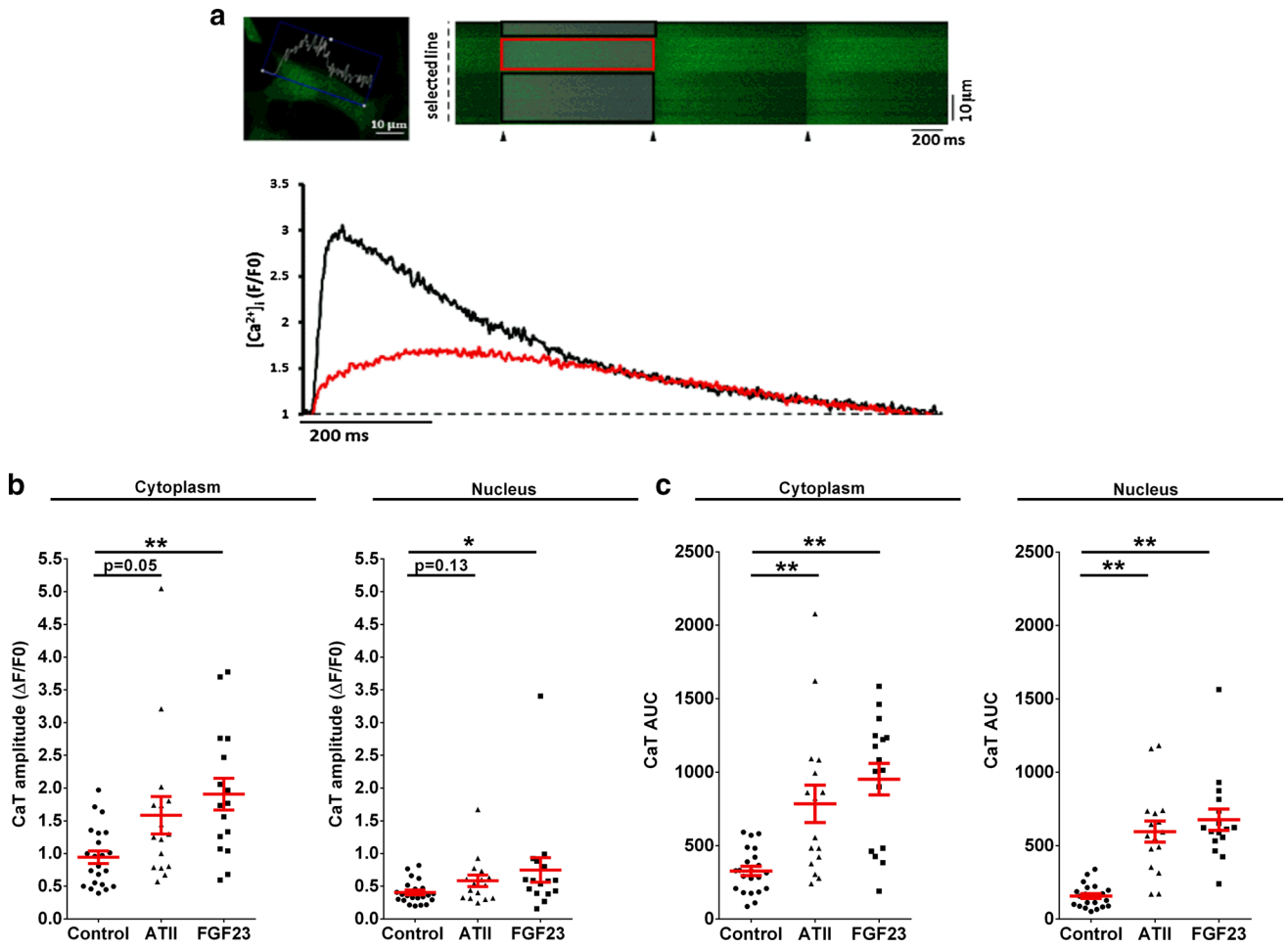

Fig. 2 Effect of acute treatment with FGF23 and ATII on Ca^{2+} transient. **a** Simultaneous confocal line-scan imaging of cytoplasmic and nucleoplasmic CaTs (above) recorded in a field-stimulated (1 Hz) cardiomyocyte (stimulation is marked by the black triangles). The traces (below) represent $[Ca^{2+}]_i$ expressed as normalized changes of fluo-4 fluorescence (F/F0) in the cytoplasm (black) and nucleus (red). **b** Ca^{2+} transient peak amplitude after ATII (triangle) and FGF23 (square) treatment vs. control NRVMs (circle) for 15–90 min in the cytoplasm (left) and in the nucleus (right). **c** Ca^{2+} transient AUC in cytoplasm (left) and in nucleus (right) after both the treatments vs. control NRVMs (circle) (each symbol represents 1 cell; mean ± SEM; $n > 15$ cells for each group and region; $N = 3$ isolations of NRVMs; $^*P < 0.05$, $^{**}P < 0.01$, compared with corresponding vehicle-treated control; Kruskal–Wallis followed by Dunn's test)

whereas losartan alone did not have significant effect on CaT amplitude in NRVMs vs. vehicle-treated control cells in cytoplasm (0.73 ± 0.13 and 0.76 ± 0.07 in losartan-treated and control, n ≥ 8 cells) and nucleus (0.38 ± 0.07 and 0.30 ± 0.03 in losartan-treated and control). CaT AUC in NRVMs was also not affected by losartan in cytoplasm (253.4 ± 45.6 and 252 ± 17.3 in losartan-treated and control; n ≥ 8 cells) and nucleus (153.2 ± 24.9 and 118.3 ± 11.5 in losartan-treated and control). Furthermore, pre-treatment with losartan significantly attenuated the FGF23-induced increase in cardiomyocyte size (Fig. 4c) and mitigated FGF23-induced upregulation of hypertrophy gene, ACTA-1 (Fig. 4d).

Thus, inhibition of ATII/AT1R signaling leads to blocking of FGF23-induced cellular hypertrophy in ventricular cardiomyocytes.

FGF23 stimulates expression of intracellular ATII in NRVMs

Earlier studies have shown that ATII can be produced intracellularly in cardiomyocytes in response to different stimuli [16]. Here, we examined whether FGF23 induces a rise in expression of ATII in cardiomyocytes. Induction of intracellular ATII expression by FGF23 in NRVMs was measured using immunofluorescence. High extracellular glucose, previously known to induce production of ATII [16], was used as a positive control. FGF23 significantly increased % cell area expressing ATII in NRVMs after 90 min of treatment (5.9 ± 0.3% of cell area vs. 2.7 ± 0.2% in vehicle-treated control, Fig. 5b), a time-point when FGF-induced Ca^{2+} changes were observed. A time-dependent increase in ATII expression was observed at 24 h in FGF23-treated

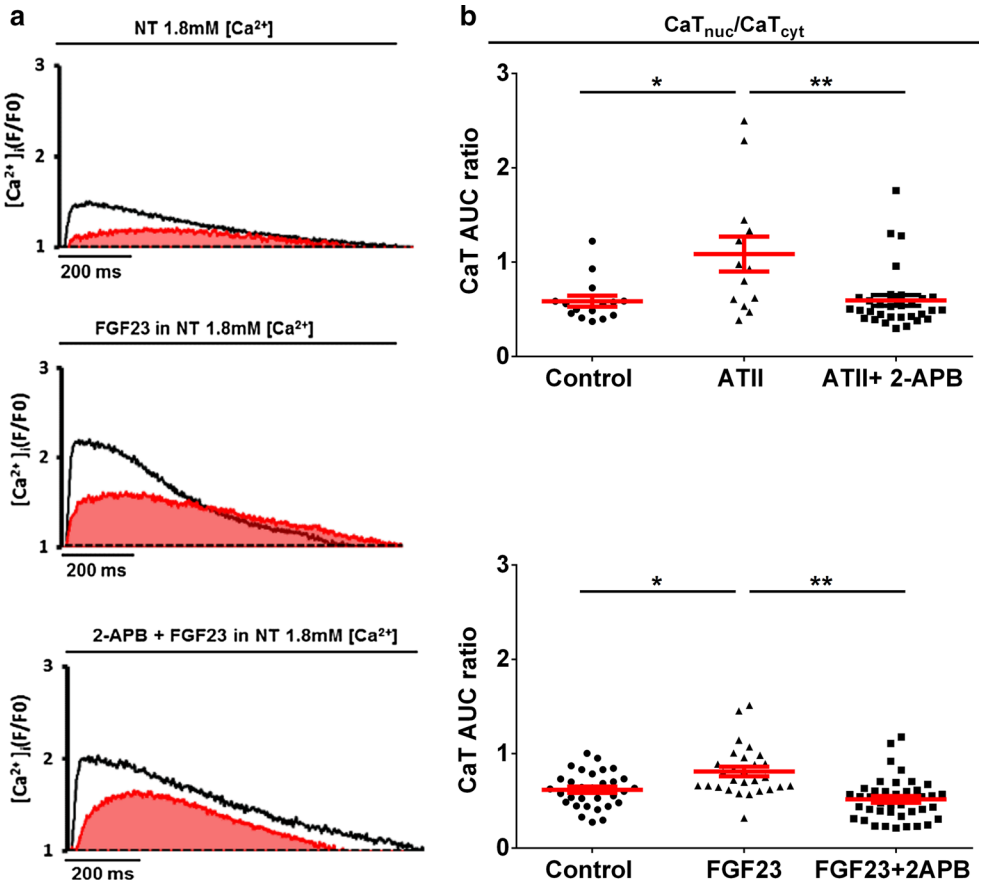

Fig. 3 Effect of 2-APB on FGF23-evoked active Ca^{2+} release in the nucleus. **a** Typical examples of original recordings of electrically stimulated Ca^{2+} transients in the vehicle-treated control cell (above), cell treated with FGF23 (middle), and the cell pre-treated with 2-APB for 30 min before FGF23 stimulation (below). The area covered in under the nuclear CaT (red) is considered as nuclear CaT AUC. **b** Effect of 2-APB (square) on Ca^{2+} transient AUC in nucleus normalized to the corresponding cytoplasmic Ca^{2+} transient AUC (CaT AUC ratio) in NRVMs treated with ATII (above) and FGF23 (below) (triangle) (each symbol represents 1 cell; mean ± SEM; $n > 10$ cells for each group and region; $N = 4$ isolations of NRVMs; $^*P < 0.05$, $^{**}P < 0.01$; Kruskal–Wallis followed by Dunn's test)

cardiomyocytes with (13.6 ± 1.6%) compared with vehicle-treated control cells (3.24 ± 0.5%) (Fig. S5). As expected, high glucose had a significant effect on intracellular ATII levels both, at 90 min and 24 h (18.8 ± 1.5 and 8.3 ± 1.3% cell area, respectively). Overall, these observations suggest that FG23 induces intracellular synthesis of ATII in ventricular cardiomyocytes.

FGF23-induced secretion of ATII from NRVMs

As ATII itself has an important role in inducing hypertrophy in cardiomyocytes and since we found that FGF23 could induce intracellular synthesis of ATII, we sought to determine if the induced ATII is secreted extracellularly in response to the FGF23 treatment. To detect the secretion of FGF23-upregulated ATII, we performed mass spectrometry analysis of the conditioned medium after treating NRVMs with FGF23 for 24 h and compared it with media obtained from vehicle-treated control NRVMs. Qualitative results were gathered from MALDI-IMS as represented in the mass spectra (Fig. 6a, b). The initial inspection of the mass spectra revealed a number of prominent peaks found between *m/z* 800–3000 with the intensity and profile clearly altered between the two groups. In Fig. 6c, overlapped representative mass spectra (*m/z* range 1044–1054) evidently showed the presence of a peak of ATII peptide (*m/z* 1046.562) in the supernatant collected from FGF23-treated NRVMs. This ATII peak was absent in the supernatant collected from vehicle-treated control NRVMs.

These results suggest that FGF23 not only induces intracellular synthesis of ATII in cardiomyocytes but also stimulates extracellular release of the ATII peptide, albeit on long-term treatment.

Discussion

In this study, we explored the effects of FGF23 on intracellular Ca^{2+} homeostasis and signaling related to cellular hypertrophy. First, we show that, similar to ATII, FGF23 induces hypertrophy possibly via common Ca^{2+}-mediated signaling pathway. Second, we provide evidence, suggesting that hypertrophy induced by FGF23 is associated with CAMKII-HDAC4 signaling via the IP3-dependent nuclear Ca^{2+} release (IICR). Third, we demonstrate that ATII/AT1R-antagonist losartan attenuates FGF23-induced effects on cardiomyocyte hypertrophy and Ca^{2+} signaling. Finally, we showed that FGF23 enhances ATII expression and secretion in cardiomyocytes, suggesting a cross talk between FGF23- and ATII-mediated signaling in cardiomyocytes.

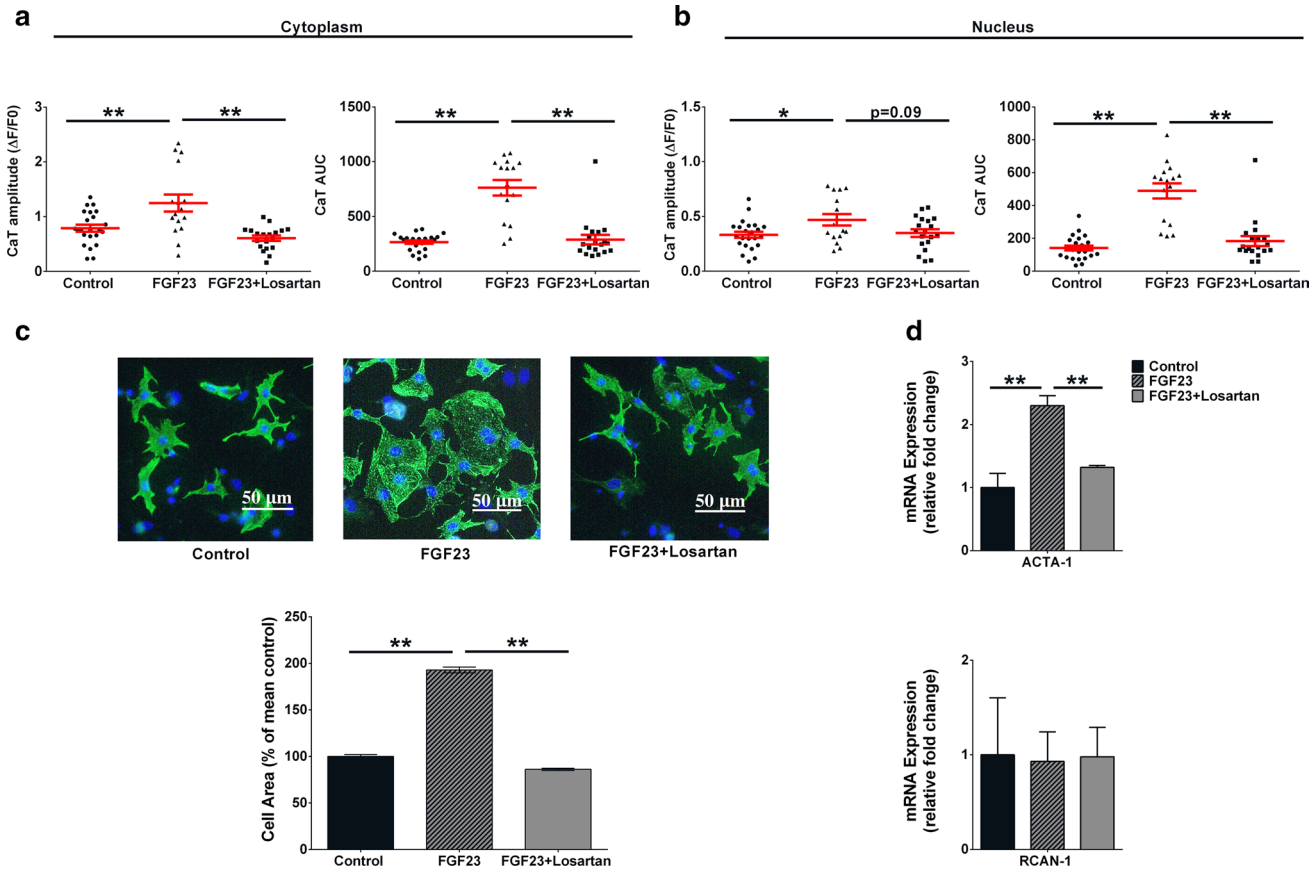

Fig. 4 Effect of Losartan (1 µM) on FGF23-induced Ca^{2+} release and hypertrophy. **a** Effect of 30-min pre-treatment of losartan (square) on Ca^{2+} transient peak amplitude (left) and AUC (right) in cytoplasm and **b** in nucleus of FGF23 -treated NRVMs (mean ± SEM; $n > 15$ cells for each group and region; $N = 3$ isolations of NRVMs; $^{*}P < 0.05$, $^{**}P < 0.01$, compared with corresponding control). **c** Representative images (above) of isolated NRVMs for each condition after immunocytochemical analysis using antibodies to cardiomyocyte-specific Desmin (green), DAPI (blue) was used to identify nuclei (scale bar: 50 µm). The bar graph (below) represents relative percentage change in cell area compared to vehicle-treated control cells (black) in NRVMs treated with FGF23 (pattern) for 48 h or after 30 min pre-treatment of losartan (grey) (mean ± SEM; $n > 1000$ cells per group; $N = 3$ isolations of NRVMs; $^{*}P < 0.05$, $^{**}P < 0.01$; Kruskal–Wallis followed by Dunn's test). **d** Compared to control cells (black), expression of genes ACTA-1 (above) and RCAN-1 (below) at 6 h of FGF23 treatment (pattern) or after 30 min pre-treatment of losartan (grey) (mean ± SEM; $N = 4$ independent isolations quantified by RT-PCR normalized to GAPDH gene expression; $^{**}P < 0.01$; unpaired *t* test or Mann–Whitney *U* test)

In preclinical models as well as in patients with chronic kidney disease, elevated serum concentrations of FGF23 are independently associated with LVH. The expression levels of FGF receptor (FGFR4), calcineurin, and NFAT are increased in myocardial tissue of patients with CKD and correlate with the presence of LVH, suggesting activation of an FGF23-driven pro-hypertrophic pathway in these patients [21]. Likewise, direct LV myocardial delivery of FGF23 induces LVH in mice. Along with in vivo hypertrophy, a significant increase in the FGF23-induced cross-sectional surface area of cardiomyocytes and hypertrophic genes expression was observed in cultured cardiomyocytes [8]. We chose NRVM as a model to allow quantitative recordings of subcellular Ca^{2+} transients in controlled extracellular conditions. While this approach ignores additional mechanical, neurohumoral, and paracrine triggers, it allows us to dissect single receptor-mediated signaling pathways. We chose a model of healthy cardiomyocytes, because our aim was to study the early adaptation to hypertrophic triggers. NRVM are less differentiated, but yet fully functional, contracting cardiomyocytes. NRVM are much more susceptible to hypertrophic triggers and growth than adult terminally differentiated cardiomyocytes in vitro. While NRVMs are in a premature state with respect to Ca^{2+}-handling, this bears resemblance to long-term cultured as well as diseased adult cardiomyocytes where there is a loss of t-tubule organization and web-like arrangement of contractile proteins [22]. Nonetheless, functional signaling pathways for ATII and FGF23 have been demonstrated previously in NRVM [8].

In the present study, we confirmed direct hypertrophic effects of FGF23 in cardiomyocytes, and found them

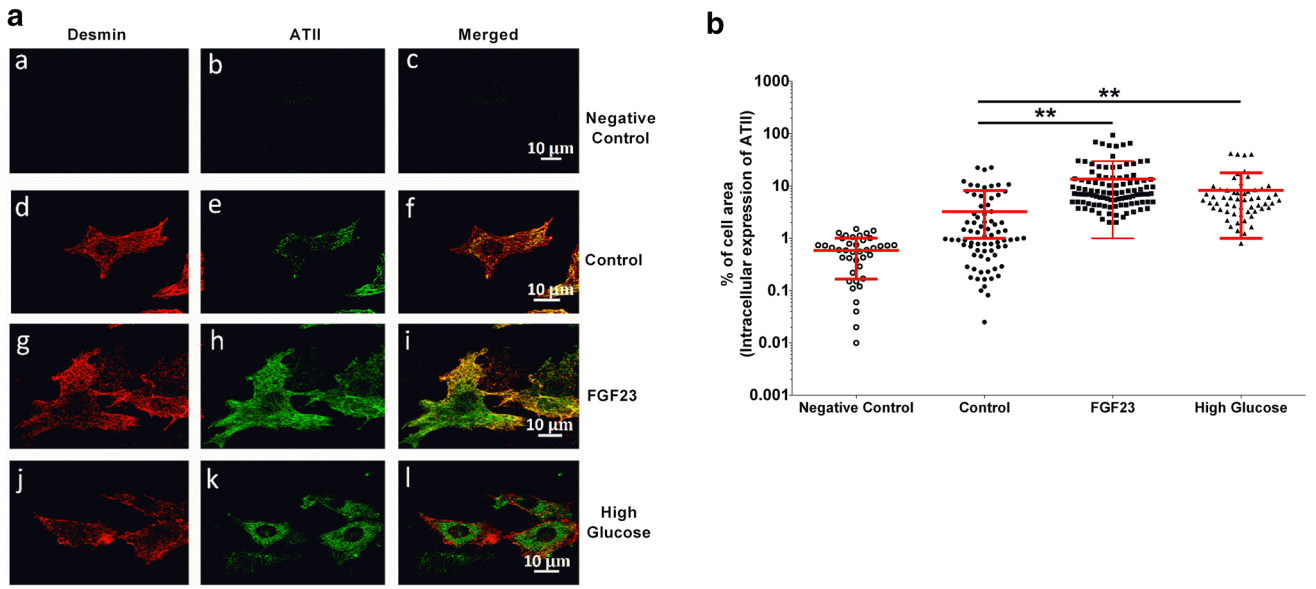

Fig. 5 Expression of intra-cardiac ATII induced by FGF23 treatment for 90 min. **a** Representative confocal images of NRVM immunofluorescence in negative control (a–c), vehicle-treated control (d–f), FGF23 (g–i), and high glucose (25 mM) (j–l) conditions after 90 min of treatment (scale bar: 10 µm). **b** Quantitative analysis by thresholding (see "Methods" for details) of ATII-specific cellular immunofluorescence for all the treatments at 90 min (each symbol represents 1 cell; mean ± SD; $n_{cells} \geq 40$ for each group; $N \geq 3$ isolations of NRVMs; $^{**}P < 0.01$, compared with corresponding vehicle-treated control cells; Kruskal–Wallis followed by Dunn's test)

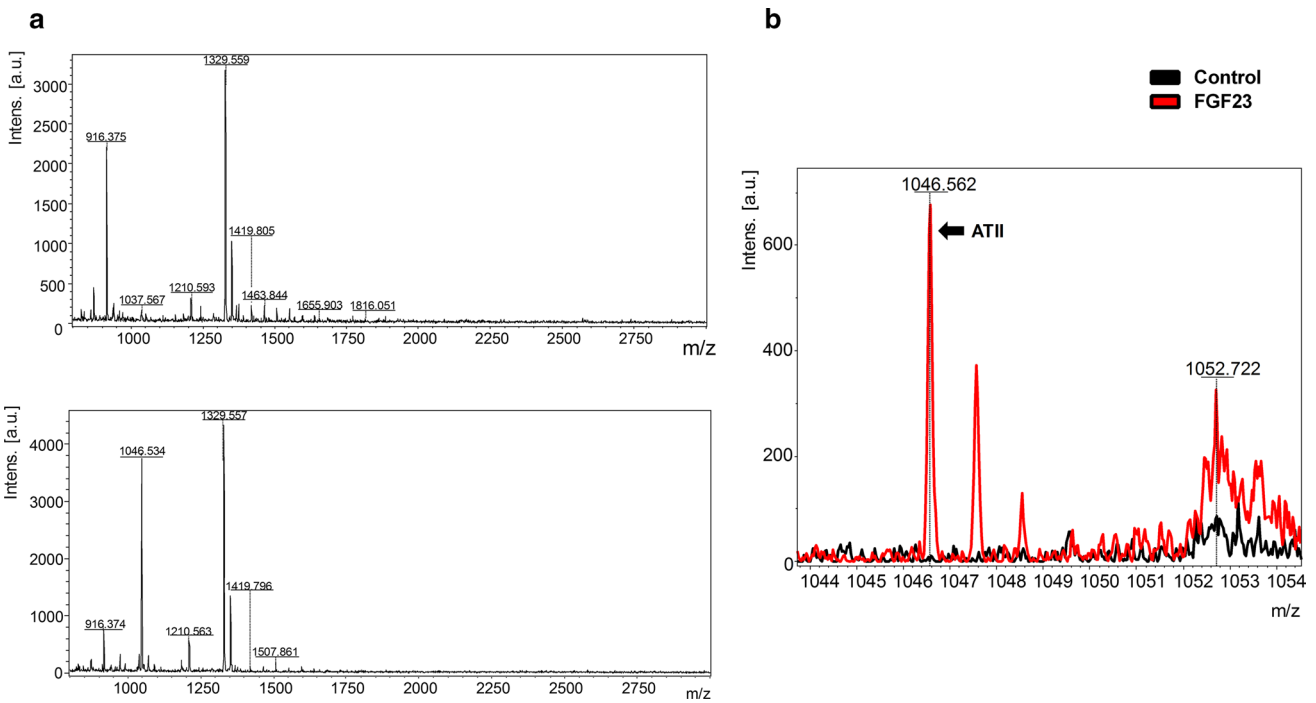

Fig. 6 Detection of secreted ATII from NRVM exposed to FGF23 by mass spectrometry. **a** Representative mass spectra (*m/z* 800–3000) of conditioned media samples from vehicle-treated control NRVMs (above) and FGF23 treated NRVMs (below) for 24 h. **b** Superimposed representative mass spectra (*m/z* 1044–1054) were extracted and amplified from full mass chromatogram of conditioned medium from 24 h FGF23 treated NRVMs (red) and control NRVMs (black)

comparable to ATII with respect to effects on cell size and early activation of markers genes of LVH and fibrosis (Fig. 1a, b).

ATII, an important mediator of the RAAS cascade, is a major trigger of cardiac hypertrophy. In cardiomyocytes, ATII acts via the angiotensin II receptor type 1 (AT1R), a classical G-protein-coupled receptor (GPCR). Downstream of GPCR, IICR plays a pivotal role in regulating cardiac hypertrophy [1]. IP3-mediated enhanced intracellular nuclear Ca^{2+} and activation of Ca^{2+}-sensors such as Ca^{2+}/calmodulin-dependent protein kinase II (CaMKII) trigger the development of ATII-induced cardiac hypertrophy [23]. CaMKII specifically regulates the phosphorylation (Ser-632) of anti-hypertrophic transcription repressor histone deacetylase 4 (HDAC4) [24, 25]. As a result, HDAC4 is exported from the nucleus to cytoplasm, where it no longer serves anti-hypertrophic functions against transcription factors MEF2 and SRF, resulting in activation of hypertrophic gene programs that are controlled by these transcription factors [26, 27].

FGF23, on the other hand, acts on cardiomyocytes by binding to FGFR4, which belongs to a different class of cell surface receptors, i.e., receptor tyrosine kinases (RTK). Activation of FGFR4 is required for the FGF23-induced hypertrophy as FGFR4-specific blocking antibody prevents FGF23-induced cellular hypertrophy in NRVMs. These results are consistent with the in vivo studies demonstrating an absence of hypertrophy induced by FGF23 in $FGFR4^{-/-}$ mice [28].

FGF23 also has profound effects on cytosolic Ca^{2+} regulation in cardiomyocytes. Exposure of primary cardiomyocytes to FGF23 increases cytosolic $[Ca^{2+}]_i$ significantly (Fig. 2b, c; [9]), and similar to ATII, this leads to cardiomyocyte hypertrophy via the activation of the calcineurin-NFAT signaling pathway [8, 28]. However, ATII also activates CAMKII/HDAC-4 hypertrophic signaling via IICR-mediated nuclear Ca^{2+} elevation. With immunoblotting experiments, we found that FGF23 too increase CAMKII-mediated HDAC-4 phosphorylation (Fig. 1c), suggesting nuclear Ca^{2+} involvement in FGF23-induced cellular hypertrophy.

We and others have previously shown that the nucleus surrounded by the nuclear envelope (NE) forms a compartment with differentially regulated Ca^{2+} signaling [3]. While the nucleus participates in global cytosolic Ca^{2+} changes during excitation–contraction coupling (ECC), amplitude and kinetics of nuclear Ca^{2+} transients may differ from the cytosols. This, in part, can be explained by the additional release of Ca^{2+} into the nucleus from the NE via IP3-receptors (IICR) [29, 30]. This excess nuclear Ca^{2+} has been shown to be important for hypertrophic signaling [3, 31]. While our results indicate an increase in nuclear $[Ca^{2+}]$ and activation of Ca^{2+}-dependent nuclear signaling (HDAC4), where nuclear $[Ca^{2+}]$ is sensitive to both the IP3 blockers (see below), the Ca^{2+}-dependent fluorescence signal is also influenced by the dye properties in the respective compartments [18]. The ratio of Ca^{2+} concentrations in nucleus and cytosol in the present study is, therefore, a surrogate marker for differential changes in these compartments but not necessarily a ratio in absolute terms.

The role of IICR in FGF23-mediated hypertrophy has not been tested so far. We chose to study paced cardiomyocytes, as the duality of large amounts of Ca^{2+}-induced Ca^{2+} release (CICR) during ECC and local Ca^{2+} signaling (IICR) for Ca^{2+}-dependent hypertrophic remodeling is an important feature of differentiated beating cardiomyocytes. In the present study, we show that, similar to ATII, excess nuclear $[Ca^{2+}]$ via IICR is involved in FGF23-induced hypertrophy (Fig. 3a, b; S4). While limited specificity of all the current IP3R blockers warrant caution in the interpretation of pharmacological IP3R inhibition, two different compounds, 2-ABP and xestospongin C, yielded similar results. Even though IP3 signaling may have a more prominent role in neonatal vs. (healthy) adult rat cardiomyocytes [32], IP3-dependent signaling is similarly relevant for cardiac hypertrophy in adult cardiomyocytes [30].

Angiotensin receptor blockers (ARBs) are drugs which selectively block AT1R by directly preventing the binding of ATII and hence impede downstream maladaptive signaling [33]. Numerous clinical trials with ARBs have suggested that this class of drugs is most effective in LVH regression [34, 35].

Based on this rationale, we used ATII as a reference Ca^{2+}-regulated hypertrophy trigger for comparison with FGF23.

ATII modulate $[Ca^{2+}]_i$ and influence myocardium both in vivo and in vitro. ATII on acute treatment not only increases the three intracellular Ca^{2+} parameters of cytoplasmic-resting intracellular Ca^{2+}, Ca^{2+} sparks, and wave frequency but also has a specific effect on nuclear Ca^{2+} in cardiomyocytes [36]. ATII increases nuclear systolic and diastolic Ca^{2+} vs. vehicle-treated cardiomyocytes and this effect gets aggravated in LVH mice model [3]. As stated earlier, IP3 is known to regulate nuclear CaTs by localized Ca^{2+} release via IP3R located on the inner membrane of the nuclear envelope [3, 37]. Stimulation of AT1R, via classical cytosolic Gq signaling, involves the activation of phospholipase C-β (PLC-β) that leads to release of IP3 in the cytosol. The IP3-mediated perinuclear Ca^{2+} increase is involved in the expression of hypertrophic marker genes via translocation of histone deacetylases and activation of Ca^{2+}-regulated transcription factors leading to hypertrophy of the heart [3, 19, 27, 38, 39]. Essentially, ATII stimulation generates [IP3] which excites local nuclear Ca^{2+} release to induce LVH [37, 40, 41].

The distinct features of nuclear IP3-IP3R signaling include prolonged and sustained nuclear CaT response along

with greater basal spark rate and higher sparks due to IP3 on GPCR stimulation changing the nuclear Ca^{2+} dynamics [42]. Our Ca^{2+} imaging experiments demonstrated a similar increase in nuclear along with cytoplasmic CaT AUC in ATII-treated cardiomyocytes (Fig. 2b, c). However, we found significantly more cells with nuclear sparks in the ATII treatment group vs. vehicle-treated control group (Fig. S2b). In parallel experiments, FGF23-induced comparable augmentation in nuclear CaT (Fig. 2b, c), along with similar increase in cells with nuclear sparks in FGF23 treatment group (Fig. S2a, b). Furthermore, spark frequency within the nucleus was significantly increased in FGF23-treated cells vs. control cells (Fig. S2c). Thus, like ATII, the rise in local nuclear Ca^{2+} release and CaT may be involved in instigating FGF23-induced hypertrophy in NRVMs.

Our results emphasize that both ATII and FGF23 induce cellular hypertrophy via a common Ca^{2+}-mediated signaling pathway in cardiomyocytes. Based on these results, next, we tested the hypothesis that FGF23–FGFR4 may act upstream of the ATII pathway.

To investigate this hypothesis, we used losartan, a clinically established AT1R antagonist and competitive inhibitor of ATII. Losartan blocks the rapid internalization of AT1R upon agonist stimulation, thus inhibiting the induction of pathological signaling by ATII. In vivo, it inhibits hypertrophy induced by ATII in cardiomyocytes from spontaneously hypertensive rat models as well as in individual cardiomyocytes under stress conditions like mechanical stretch [43, 44].

Strikingly, we observed that losartan inhibited changes in intracellular Ca^{2+} homeostasis induced by FGF23. Our data showed that AT1R-inhibition abrogates FGF23-stimulated changes in CaT with respect to amplitude and AUC in the cytoplasm (Fig. 4a) as well as the nucleus (Fig. 4b). Next, we observed attenuation of hypertrophic cell size increase and ACTA-1 upregulation induced by FGF23 (Fig. 4c, d).

Hence, AT1R blocker losartan not only blocks FGF23-induced Ca^{2+} transients' changes but also the FGF23 mediated cellular hypertrophy (Fig. 4c, d), suggesting that Ca^{2+}-mediated hypertrophic signaling in response to FGF23 in our model depends on ATII signaling. Our data support our main hypothesis that FGF23 and ATII share downstream IP3-dependent signaling pathways. In contrast, in the present study, we did not aim to exclude that FGF23 in other conditions and time-periods does modulate Ca^{2+} homeostasis in cardiomyocytes as has been reported earlier [9]. Overall, these results indicate the possible involvement of ATII–AT1R activation in FGF23-induced maladaptive signaling in cardiomyocytes.

Multiple studies have confirmed that cardiomyocytes produce and secrete cardiac ATII in response to maladaptive triggers like mechanical stretch, high glucose, and catecholamines [16, 45]. Cardiomyocytes express the precursors and enzymes like angiotensinogen, angiotensin-converting enzyme (ACE), chymase, and renin required for ATII synthesis [45]. Recent reports have suggested a molecular basis for such cross talks. ATII can act as an intracrine peptide in cardiomyocytes and regulates hypertrophic Ca^{2+} signaling from an intracellular location in cardiomyocytes via cognate nuclear AT1Rs [46–48].

We next assess if FGF23 induces synthesis of ATII and whether it further leads to secretion of ATII. Remarkably, the application of FGF23 acutely alters the intracellular expression of ATII in cardiomyocytes. We observed FGF23-induced sustained increase of ATII levels in cardiomyocytes after, as early as, 90 min (Fig. 5) and at 24 h (Fig. S5) as compared to vehicle-treated control cells. Furthermore, we confirmed FGF23-induced secretion of ATII from NRVMs using mass spectrometry, which was absent for control NRVMs (Fig. 6). These results suggest that, on FGF23 treatment, ATII peptide was synthesized in the secretory pathway possibly involving ACE in NRVMs [49]. By and large, our results indicate that FGF23-induced activation of ATII synthesis, secretion, and signaling which potentially acts as an autocrine signal to trigger maladaptive hypertrophic signaling in ventricular cardiomyocytes.

In conclusion, the evidence collected in this study does imply that ATII is the initial mediator of the FGF23-triggered hypertrophic response in cardiomyocytes. Although, it is well established that FGF23/FGFR4 pathway causes cardiac hypertrophy [28]. The convergence of FGF23 and ATII signaling might be required for FGF23-induced cardiomyocyte hypertrophy. As summarized in Fig. 7, FGF23 activates ATII signaling pathway by an increase of ATII expression and its secretion in cardiomyocytes. Simultaneously, there is an IP3-mediated Ca^{2+} release from nucleoplasm on FGF23 stimulation, which mediates nuclear Ca^{2+}-CAMKII-HDAC4-dependent hypertrophic signaling in cardiomyocytes. Cooperatively, both events might play an important role in cellular hypertrophy triggered by FGF23.

Potential clinical relevance

Cardiac hypertrophy is a maladaptive response of the heart and a therapeutic target in the presence of pathological triggers such as arterial hypertension [50]. FGF23 correlates with increased incidence and prevalence of LVH [8], which has attributed to its stimulating effects on the RAAS at the level of the kidney as well as to its direct hypertrophic effects on the heart [51, 52]. Here, we provide evidence that FGF23 may also stimulate local ATII signaling in cardiac myocytes. Thus, patients with activated FGF23 signaling as reflected by increased FGF23 serum levels (as seen in patients with chronic kidney disease) may respond particularly favorably to ATII-based treatments (ARBs), suggesting a personalized approach to alleviate LVH in these high-risk populations.

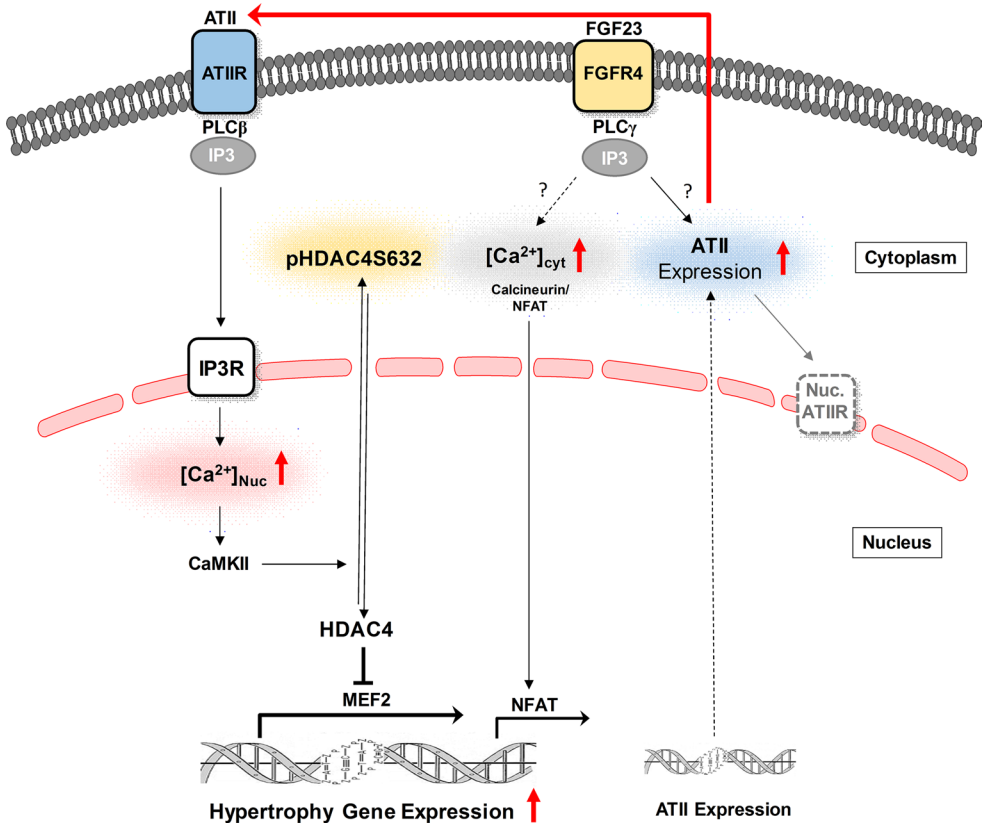

Fig. 7 Crosstalk between Ca^{2+}-mediated hypertrophic signaling by ATII and FGF23 in cardiomyocytes. Schematic diagram depicting the proposed activation of ATII signaling pathway by which FGF23/FGFR4 stimulates cardiac hypertrophy. Current studies support a model whereby FGF23 activates expression and secretion of ATII from cardiomyocytes, which, in an autocrine manner, lead to the subsequent stimulation of IP3-nuclear Ca^{2+}-CAMKII-HDAC4 pathway resulting in cellular hypertrophy. *ATII* angiotensin II, *ATIIR* angiotensin type 1 receptor, *FGF23* fibroblast growth factor-23, *FGFR4* fibroblast growth factor receptor 4, *PLC-β/γ* phospholipase C-β/γ, *IP3* inositol 1, 4, 5-triphosphate, $[Ca^{2+}]_{cyt}$ cytoplasmic calcium, $[Ca^{2+}]_{nuc}$ nuclear calcium, *CAMKII* Ca^{2+}/calmodulin-dependent protein kinase II, *HDAC-4* histone deacetylase-4, *pHDAC4S632* phophorylated HDAC4 at site Serine 632, *MEF-2* myocyte enhancer factor-2, *NFAT* nuclear factor of activated T cells, *Nuc.ATIIR* nuclear angiotensin type 1 receptor

Acknowledgements K.M. was supported by the Ph.D. Program Molecular Medicine at the Medical University of Graz.

Compliance with ethical standards

Conflict of interest The authors declare that they have no competing interests.

References

1. Nakayama H, Bodi I, Maillet M, Desantiago J, Domeier TL, Mikoshiba K, Lorenz JN, Blatter LA, Bers DM, Molkentin JD (2010) The IP3 receptor regulates cardiac hypertrophy in response to select stimuli. Circ Res 107:659–666. https://doi.org/10.1161/CIRCRESAHA.110.220038
2. Dickhout JG, Carlisle RE, Austin RC (2011) Interrelationship between cardiac hypertrophy, heart failure, and chronic kidney disease: endoplasmic reticulum stress as a mediator of pathogenesis. Circ Res 108:629–642. https://doi.org/10.1161/CIRCRESAHA.110.226803
3. Ljubojevic S, Radulovic S, Leitinger G, Sedej S, Sacherer M, Holzer M, Winkler C, Pritz E, Mittler T, Schmidt A, Sereinigg M, Wakula P, Zissimopoulos S, Bisping E, Post H, Marsche G, Bossuyt J, Bers DM, Kockskämper J, Pieske B (2014) Early remodeling of perinuclear Ca^{2+} stores and nucleoplasmic $Ca2^{2+}$ signaling during the development of hypertrophy and heart failure. Circulation 130:244–255. https://doi.org/10.1161/CIRCULATIONAHA.114.008927
4. Dewenter M, Von Der Lieth A, Katus HA, Backs J (2017) Calcium signaling and transcriptional regulation in cardiomyocytes. Circ Res 121:1000–1020. https://doi.org/10.1161/CIRCRESAHA.117.310355
5. Higazi DR, Fearnley CJ, Drawnel FM, Talasila A, Corps EM, Ritter O, McDonald F, Mikoshiba K, Bootman MD, Roderick HL (2009) Endothelin-1-stimulated InsP3-induced Ca^{2+} release is a nexus for hypertrophic signaling in cardiac myocytes. Mol Cell 33:472–482. https://doi.org/10.1016/j.molcel.2009.02.005
6. Garcia MI, Karlstaedt A, Amione-Guerra J, Youker KA, Taegtmeyer H, Boehning D (2016) Functionally redundant control of cardiac hypertrophic signaling by inositol 1,4,5-trisphosphate receptors. J Mol Cell Cardiol 112:95–103. https://doi.org/10.1101/075044

7. Nabeshima Y (2008) The discovery of α-Klotho and FGF23 unveiled new insight into calcium and phosphate homeostasis. Cell Mol Life Sci 65:3218–3230. https://doi.org/10.1007/s00018-008-8177-0
8. Faul C, Amaral AP, Oskouei B, Hu M, Sloan A, Isakova T, Gutiérrez OM, Aguillon-prada R, Lincoln J, Hare JM, Mundel P, Morales A, Scialla J, Fischer M, Soliman EZ, Feldman HI, Sutton J, Ojo A, Gadegbeku C, Seno G, Marco D, Reuter S, Kentrup D, Tiemann K, Brand M, Hill JA, Moe OW, Kuro-o M, Kusek JW, Keane MG, Wolf M (2011) FGF23 induces left ventricular hypertrophy. J Clin Investig. https://doi.org/10.1172/jci46122.ease
9. Touchberry CD, Green TM, Tchikrizov V, Mannix JE, Mao TF, Carney BW, Girgis M, Vincent RJ, Wetmore LA, Dawn B, Bonewald LF, Stubbs JR, Wacker MJ (2013) FGF23 is a novel regulator of intracellular calcium and cardiac contractility in addition to cardiac hypertrophy. AJP Endocrinol Metab 304:E863–E873. https://doi.org/10.1152/ajpendo.00596.2012
10. Kao Y-H, Chen Y-C, Lin Y-K, Shiu R-J, Chao T-F, Chen S-A, Chen Y-J (2014) FGF-23 dysregulates calcium homeostasis and electrophysiological properties in HL-1 atrial cells. Eur J Clin Investig 44:795–801. https://doi.org/10.1111/eci.12296
11. Bisping E, Ikeda S, Sedej M, Wakula P, McMullen JR, Tarnavski O, Sedej S, Izumo S, Pu WT, Pieske B (2012) Transcription factor GATA4 is activated but not required for insulin-like growth factor 1 (IGF1)-induced cardiac hypertrophy. J Biol Chem 287:9827–9834. https://doi.org/10.1074/jbc.M111.338749
12. Kreusser MM, Lehmann LH, Keranov S, Hoting MO, Oehl U, Kohlhaas M, Reil JC, Neumann K, Schneider MD, Hill JA, Dobrev D, Maack C, Maier LS, Gröne HJ, Katus HA, Olson EN, Backs J (2014) Cardiac CaM kinase II genes δ and γ contribute to adverse remodeling but redundantly inhibit calcineurin-induced myocardial hypertrophy. Circulation 130:1262–1273. https://doi.org/10.1161/CIRCULATIONAHA.114.006185
13. Hohendanner F, Ljubojević S, MacQuaide N, Sacherer M, Sedej S, Biesmans L, Wakula P, Platzer D, Sokolow S, Herchuelz A, Antoons G, Sipido K, Pieske B, Heinzel FR (2013) Intracellular dyssynchrony of diastolic cytosolic [Ca^{2+}] decay in ventricular cardiomyocytes in cardiac remodeling and human heart failure. Circ Res 113:527–538. https://doi.org/10.1161/CIRCRESAHA.113.300895
14. Heinzel FR, Bito V, Biesmans L, Wu M, Detre E, Von Wegner F, Claus P, Dymarkowski S, Maes F, Bogaert J, Rademakers F, D'Hooge J, Sipido K (2008) Remodeling of T-tubules and reduced synchrony of Ca^{2+} release in myocytes from chronically ischemic myocardium. Circ Res 102:338–346. https://doi.org/10.1161/CIRCRESAHA.107.160085
15. Lederer WJ, Introduction I, Sparks C, Sparks D, Terminology G, Ca C, Morphology VS, Amplitude A, Width B, Kinetics C, Autonomy D, Overview A, Cicr C, Ca L (2008) SparkMaster: automated calcium spark analysis with ImageJ. Physiol Rev 88:1491–1545. https://doi.org/10.1152/physrev.00030.2007
16. Singh VP, Le B, Bhat VB, Baker KM, Kumar R (2007) High-glucose-induced regulation of intracellular ANG II synthesis and nuclear redistribution in cardiac myocytes. Am J Physiol Heart Circ Physiol 293:H939–H948. https://doi.org/10.1152/ajpheart.00391.2007
17. Matsushima S, Kuroda J, Ago T, Zhai P, Park JY, Xie LH, Tian B, Sadoshima J (2013) Increased oxidative stress in the nucleus caused by Nox4 mediates oxidation of HDAC4 and cardiac hypertrophy. Circ Res 112:651–663. https://doi.org/10.1161/CIRCRESAHA.112.279760
18. Ljubojević S, Walther S, Asgarzoei M, Sedej S, Pieske B, Kockskämper J (2011) In situ calibration of nucleoplasmic versus cytoplasmic Ca^{2+} concentration in adult cardiomyocytes. Biophys J 100:2356–2366. https://doi.org/10.1016/j.bpj.2011.03.060
19. Plačkić J, Preissl S, Nikonova Y, Pluteanu F, Hein L, Kockskämper J (2016) Enhanced nucleoplasmic Ca^{2+} signaling in ventricular myocytes from young hypertensive rats. J Mol Cell Cardiol 101:58–68. https://doi.org/10.1016/j.yjmcc.2016.11.001
20. Bootman MD, Collins TJ, Mackenzie L, Roderick HL, Berridge MJ, Peppiatt CM (2002) 2-aminoethoxydiphenyl borate (2-APB) is a reliable blocker of store-operated Ca^{2+} entry but an inconsistent inhibitor of InsP3-induced Ca^{2+} release. FASEB J. 16:1145–1150. https://doi.org/10.1096/fj.02-0037rev
21. Leifheit-Nestler M, Siemer RG, Flasbart K, Richter B, Kirchhoff F, Ziegler WH, Klintschar M, Becker JU, Erbersdobler A, Aufricht C, Seeman T, Fischer DC, Faul C, Haffner D (2016) Induction of cardiac FGF23/FGFR4 expression is associated with left ventricular hypertrophy in patients with chronic kidney disease. Nephrol Dial Transplant 31:1088–1099. https://doi.org/10.1093/ndt/gfv421
22. Louch WE, Koivumäki JT, Tavi P (2015) Calcium signalling in developing cardiomyocytes: implications for model systems and disease. J Physiol 593:1047–1063. https://doi.org/10.1113/jphysiol.2014.274712
23. Zhang W, Qi F, Chen D-Q, Xiao W-Y, Wang J, Zhu W-Z (2010) Ca^{2+}/calmodulin-dependent protein kinase IIdelta orchestrates G-protein-coupled receptor and electric field stimulation-induced cardiomyocyte hypertrophy. Clin Exp Pharmacol Physiol 37:795–802. https://doi.org/10.1111/j.1440-1681.2010.05382.x
24. Backs J, Backs T, Neef S, Kreusser MM, Lehmann LH, Patrick DM, Grueter CE, Qi X, Richardson JA, Hill JA, Katus HA, Bassel-Duby R, Maier LS, Olson EN (2009) The isoform of CaM kinase II is required for pathological cardiac hypertrophy and remodeling after pressure overload. Proc Natl Acad Sci 106:2342–2347. https://doi.org/10.1073/pnas.0813013106
25. Kee HJ, Sohn IS, Il Nam K, Park JE, Qian YR, Yin Z, Ahn Y, Jeong MH, Bang Y-J, Kim N, Kim J-K, Kim KK, Epstein J, Kook H (2006) Inhibition of histone deacetylation blocks cardiac hypertrophy induced by angiotensin II infusion and aortic banding. Circulation 113:51–59. https://doi.org/10.1161/circulationaha.105.559724
26. Kreusser MM, Backs J (2014) Integrated mechanisms of CaMKII-dependent ventricular remodeling. Front Pharmacol. https://doi.org/10.3389/fphar.2014.00036
27. Backs J, Song K, Bezprozvannaya S, Chang S, Olson EN (2006) CaM kinase II selectively signals to histone deacetylase 4 during cardiomyocyte hypertrophy. J Clin Investig 116:1853–1864. https://doi.org/10.1172/JCI27438
28. Grabner A, Amaral AP, Schramm K, Singh S, Sloan A, Yanucil C, Li J, Shehadeh L, Hare JM, David V, Martin A, Fornoni A, Di Marco GS, Kentrup D, Reuter S, Mayer AB, Pavenst H, Stypmann J, Kuhn C, Hille S, Frey N, Leifheit-Nestler M, Richter B, Haffner D, Abraham R, Bange J, Sperl B, Ullrich A, Brand M, Wolf M, Faul C (2015) Activation of cardiac fibroblast growth factor receptor 4 causes left ventricular hypertrophy. Cell Metab 22:1020–1032. https://doi.org/10.1016/j.cmet.2015.09.002
29. Ljubojevic S, Bers DM (2016) Nuclear calcium in cardiac myocytes senka. J Cardiovasc Pharmacol 8:583–592. https://doi.org/10.1002/aur.1474.Replication
30. Wu X, Zhang T, Bossuyt J, Li X, Mckinsey TA, Dedman JR, Olson EN, Chen J, Brown JH, Bers DM (2006) Local InsP3-dependent perinuclear Ca^{2+} signaling in cardiac myocyte excitation-transcription coupling. J Clin Investig 116:675–682. https://doi.org/10.1172/jci27374.stimuli
31. Hohendanner F, Maxwell JT, Blatter LA (2015) Cytosolic and nuclear calcium signaling in atrial myocytes: IP_3-mediated calcium release and the role of mitochondria. Channels. https://doi.org/10.1080/19336950.2015.1040966
32. Louch WE, Koivumäki JT, Tavi P (2015) Calcium signalling in developing cardiomyocytes: implications for model systems and

disease. J Physiol 5935:1047–1063. https://doi.org/10.1113/jphysiol.2014.274712
33. Tamura T, Said S, Harris J, Lu W, Gerdes M (2000) Reverse remodeling of cardiac myocyte hypertrophy in hypertension and failure by targeting of the renin–angiotensin system. Circulation 102:253–259. https://doi.org/10.1161/01.cir.102.2.253
34. Cuspidi C, Negri F, Zanchetti A (2008) Angiotensin II receptor blockers and cardiovascular protection: focus on left ventricular hypertrophy regression and atrial fibrillation prevention. Vasc Health Risk Manag 4:67–73. https://doi.org/10.2147/vhrm.2008.04.01.67
35. Heinzel FR, Hohendanner F, Jin G, Sedej S, Edelmann F (2015) Myocardial hypertrophy and its role in heart failure with preserved ejection fraction. J Appl Physiol 119:1233–1242. https://doi.org/10.1152/japplphysiol.00374.2015
36. Wang R, Wang Y, Lin WK, Zhang Y, Liu W, Huang K, Terrar DA, Solaro RJ, Wang X, Ke Y, Lei M (2014) Inhibition of angiotensin II-induced cardiac hypertrophy and associated ventricular arrhythmias by a p21 activated kinase 1 bioactive peptide. PLoS One. https://doi.org/10.1371/journal.pone.0101974
37. Bootman MD, Fearnley C, Smyrnias I, MacDonald F, Roderick HL (2009) An update on nuclear calcium signalling. J Cell Sci 122:2337–2350. https://doi.org/10.1242/jcs.028100
38. Guatimosim S, Amaya MJ, Guerra MT, Aguiar CJ, Goes AM, Gomez-Viquez NL, Rodrigues MA, Gomes DA, Martins-Cruz J, Lederer WJ, Leite MF (2008) Nuclear Ca^{2+} regulates cardiomyocyte function. Cell Calcium 44:230–242. https://doi.org/10.1016/j.ceca.2007.11.016
39. Anderson ME, Brown JH, Bers DM (2011) CaMKII in myocardial hypertrophy and heart failure. J Mol Cell Cardiol 51:468–473. https://doi.org/10.1016/j.yjmcc.2011.01.012
40. Sedej S, Schmidt A, Denegri M, Walther S, Matovina M, Arnstein G, Gutschi EM, Windhager I, Ljubojević S, Negri S, Heinzel FR, Bisping E, Vos MA, Napolitano C, Priori SG, Kockskämper J, Pieske B (2014) Subclinical abnormalities in sarcoplasmic reticulum Ca^{2+} release promote eccentric myocardial remodeling and pump failure death in response to pressure overload. J Am Coll Cardiol 63:1569–1579. https://doi.org/10.1016/j.jacc.2013.11.010
41. Arantes LM, Aguiar CJ, Amaya MJ, Figueiró NCG, Andrade LM, Rocha-Resende C, Resende RR, Franchini KG, Guatimosim S, Leite MF (2012) Nuclear inositol 1,4,5-trisphosphate is a necessary and conserved signal for the induction of both pathological and physiological cardiomyocyte hypertrophy. J Mol Cell Cardiol 53:475–486. https://doi.org/10.1016/j.yjmcc.2012.06.017
42. Hohendanner F, McCulloch AD, Blatter LA, Michailova AP (2014) Calcium and IP3 dynamics in cardiac myocytes: Experimental and computational perspectives and approaches. Front Pharmacol. https://doi.org/10.3389/fphar.2014.00035
43. Ichi Sadoshima J, Xu Y, Slayter HS, Izumo S (1993) Autocrine release of angiotensin II mediates stretch-induced hypertrophy of cardiac myocytes in vitro. Cell 75:977–984. https://doi.org/10.1016/0092-8674(93)90541-w
44. Cerbai E, Crucitti A, Sartiani L, De Paoli P, Pino R, Rodriguez ML, Gensini G, Mugelli A (2000) Long-term treatment of spontaneously hypertensive rats with losartan and electrophysiological remodeling of cardiac myocytes. Cardiovasc Res 45:388–396. https://doi.org/10.1016/S0008-6363(99)00344-2
45. Malhotra R, Sadoshima J, Brosius FC, Izumo S (1999) Mechanical stretch and angiotensin II differentially upregulate the renin–angiotensin system in cardiac myocytes in vitro. Circ Res 85:137–146. https://doi.org/10.1161/01.RES.85.2.137
46. Baker KM, Chernin MI, Schreiber T, Sanghi S, Haiderzaidi S, Booz GW, Dostal DE, Kumar R (2004) Evidence of a novel intracrine mechanism in angiotensin II-induced cardiac hypertrophy. Regul Pept 120:5–13. https://doi.org/10.1016/j.regpep.2004.04.004
47. Tadevosyan A, Maguy A, Villeneuve LR, Babin J, Bonnefoy A, Allen BG, Nattel S (2010) Nuclear-delimited angiotensin receptor-mediated signaling regulates cardiomyocyte gene expression. J Biol Chem 285:22338–22349. https://doi.org/10.1074/jbc.M110.121749
48. Tadevosyan A, Xiao J, Surinkaew S, Naud P, Merlen C, Harada M, Qi X, Chatenet D, Fournier A, Allen BG, Nattel S (2017) Intracellular angiotensin-II interacts with nuclear angiotensin receptors in cardiac fibroblasts and regulates RNA synthesis, cell proliferation, and collagen secretion. J Am Heart Assoc. https://doi.org/10.1161/jaha.116.004965
49. Singh VP, Le B, Bhat VB, Baker KM, Kumar R (2007) High-glucose-induced regulation of intracellular ANG II synthesis and nuclear redistribution in cardiac myocytes. AJP Hear Circ Physiol 293:H939–H948. https://doi.org/10.1152/ajpheart.00391.2007
50. Bisping E, Wakula P, Poteser M, Heinzel FR (2014) Targeting cardiac hypertrophy: toward a causal heart failure. Therapy 64:293–305
51. Dai B, David V, Martin A, Huang J, Li H, Jiao Y, Gu W, Quarles LD (2012) A comparative transcriptome analysis identifying FGF23 regulated genes in the kidney of a mouse CKD model. PLoS One 7:1–15. https://doi.org/10.1371/journal.pone.0044161
52. de Jong MA, Mirkovic K, Mencke R, Hoenderop JG, Bindels RJ, Vervloet MG, Hillebrands J-L, van den Born J, Navis G, de Borst MH (2016) NIGRAM consortium, Fibroblast growth factor 23 modifies the pharmacological effects of angiotensin receptor blockade in experimental renal fibrosis. Nephrol Dial Transplant 32:gfw105. https://doi.org/10.1093/ndt/gfw105